Cell Reports, Volume *31*

Supplemental Information

Attenuated Epigenetic Suppression of Muscle Stem Cell Necroptosis Is Required for Efficient Regeneration of Dystrophic Muscles

Krishnamoorthy Sreenivasan, Alessandro Ianni, Carsten Künne, Boris Strilic, Stefan Günther, Eusebio Perdiguero, Marcus Krüger, Simone Spuler, Stefan Offermanns, Pablo Gómez-del Arco, Juan Miguel Redondo, Pura Munoz-Canoves, Johnny Kim, and Thomas Braun

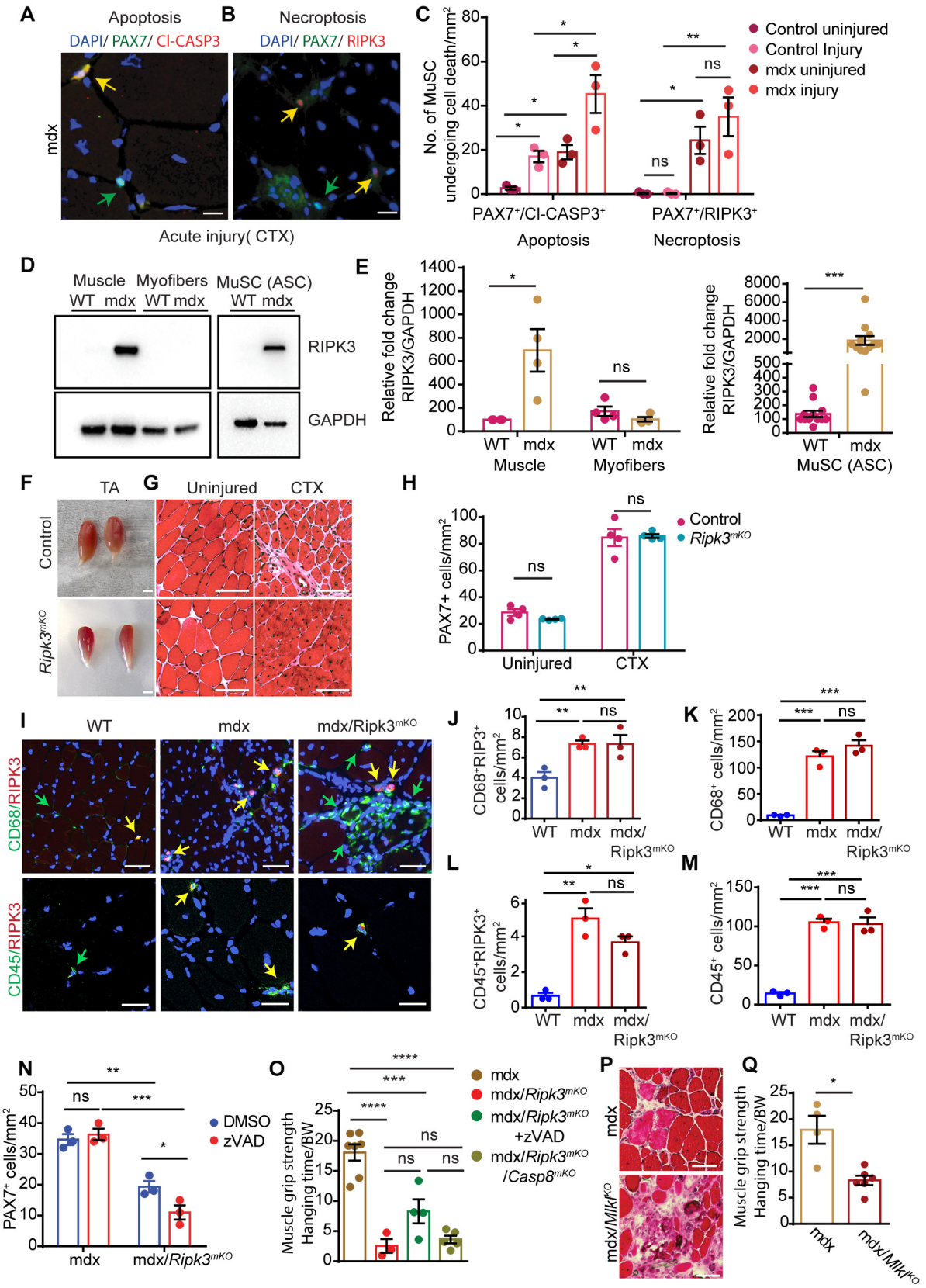
A
Apoptosis
DAPI/ PAX7/ Cl-CASP3
mdx
B
Necroptosis
DAPI/ PAX7/ RIPK3
Acute injury(CTX)
C
No. of MuSC undergoing cell death/mm2
Control uninjured
Control Injury
mdx uninjured
mdx injury
PAX7+/Cl-CASP3+
Apoptosis
PAX7+/RIPK3+
Necroptosis
D
Muscle
Myofibers
MuSC (ASC)
WT mdx
WT mdx
WT mdx
RIPK3
GAPDH
E
Relative fold change RIPK3/GAPDH
WT mdx
Muscle
WT mdx
Myofibers
Relative fold change RIPK3/GAPDH
WT mdx
MuSC (ASC)
F
TA
Control
Ripk3mKO
G
Uninjured
CTX
H
PAX7+ cells/mm2
Control
Ripk3mKO
Uninjured
CTX
I
WT
mdx
mdx/Ripk3mKO
CD68/RIPK3
CD45/RIPK3
J
CD68+RIP3+ cells/mm2
WT
mdx
mdx/ Ripk3mKO
K
CD68+ cells/mm2
WT
mdx
mdx/ Ripk3mKO
L
CD45+RIPK3+ cells/mm2
WT
mdx
mdx/ Ripk3mKO
M
CD45+ cells/mm2
WT
mdx
mdx/ Ripk3mKO
N
PAX7+ cells/mm2
DMSO
zVAD
mdx
mdx/Ripk3mKO
O
Muscle grip strength Hanging time/BW
mdx
mdx/Ripk3mKO
mdx/Ripk3mKO +zVAD
mdx/Ripk3mKO /Casp8mKO
P
mdx
mdx/Mlkl mKO
Q
Muscle grip strength Hanging time/BW
mdx
mdx/Mlkl mKO

Supplemental Figure 1: Chronic but not acute muscle injury reduces the numbers of Ripk3 deficient MuSC. Related to Figure 1 and 2.

(A-B) Immunofluorescence staining of TA muscle cross-sections from *mdx* mice two weeks after CTX injury using antibodies against PAX7 and cleaved CASP3 to detect apoptosis (A) and PAX7 and RIPK3 to detect necroptosis (B) in MuSC. Scale bar: 25 μm.

(C) Quantification of apoptotic and necroptotic cells (n=3 for each group).

(D-E) Western blot analysis of purified myofibers and MuSCs isolated from subfractionated bulk skeletal muscle from wildtype and *mdx* mice and quantified in (E), (n=3-12 for each group).

(F) Macroscopic images of $Ripk3^{mKO}$ and control TA muscles two weeks after CTX induced injury.

(G) H&E staining of cross sections from $Ripk3^{mKO}$ and control TA muscles two weeks after CTX induced injury. Scale bar (D, E): 100 μm.

(H) Quantification of $PAX7^{+}$ MuSC in control and $Ripk3^{mKO}$ mice with and without CTX injury (n=4 for each group).

(I) Immunofluorescence staining of TA muscle cross-sections from WT, *mdx* and *mdx*/$Ripk3^{mKO}$ mice using antibodies against CD68, CD45, and RIPK3. Scale bar: 25 μm.

(J-M) Quantification of $CD68^{+}$ and $CD45^{+}$ cells in TA muscle sections (n=3 for each group).

(N) Quantification of $PAX7^{+}$ MuSCs from *mdx* and *mdx*/$Ripk3^{mKO}$ mice two weeks after induction of Ripk3 inactivation and treatment with DMSO or zVAD (n=3-4 for each group; *p<0.05; **p<0.01, ***p<0.005; two-way ANOVA followed by Bonferroni post-test with alpha=5%).

(O) Quantification of muscle grip strength of *mdx*, $Ripk3^{mKO}$/*mdx*, zVAD treated $Ripk3^{mKO}$/*mdx* and $Ripk3^{mKO}/Casp8^{mKO}$/*mdx* mice (n=3-6 for each group; ***p<0.005, ****p<0.001 two-way ANOVA followed by Bonferroni post-test with alpha=5%).

(P) H&E staining of TA muscle cross-sections from *mdx* and $Mlkl^{KO}$/*mdx* mice Scale bar (D, E): 100 μm.

(Q) Quantification of muscle grip strength of *mdx* and $Mlkl^{KO}$/*mdx* mice (n=4-6 for each group; *p<0.05, two-way ANOVA followed by Bonferroni post-test with alpha=5%).

All analyses indicated across the experiments were biological replicates unless otherwise stated.

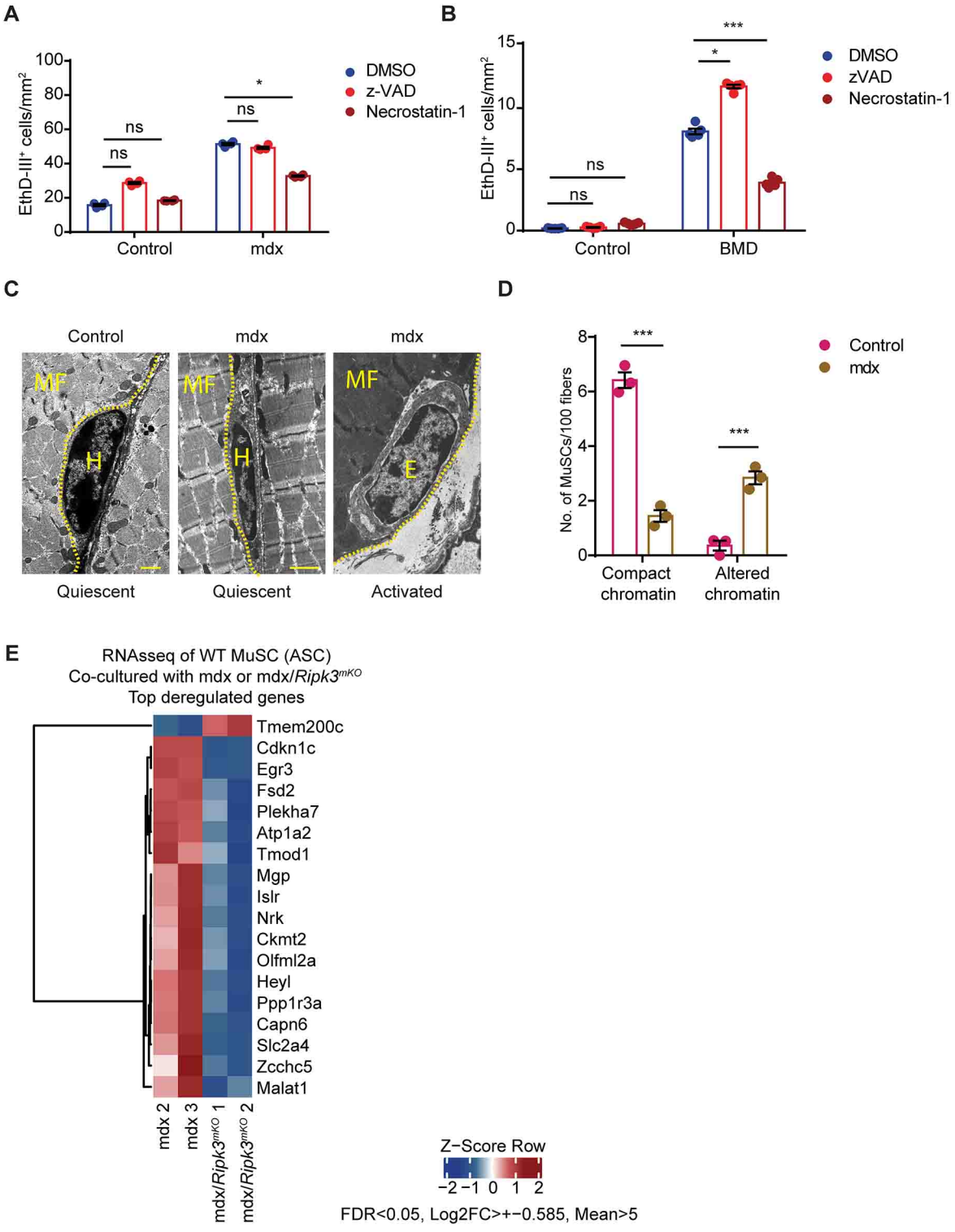

Supplemental Figure 2: MuSC from *mdx* mice and from human BMD patients are predisposed to programmed cell death. Related to Figure 3.

(A) End-point quantification of EthD-III incorporating necroptotic MuSC from control and *mdx* mice treated with z-VAD or Necrostatin-1 and DMSO (n=3 for each group; *p<0.05 two-way ANOVA followed by Bonferroni post-test with alpha=5%).

(B) End-point quantification of EthD-III incorporating necroptotic MuSC (100 hours) from control and BMD individuals treated with DMSO, z-VAD or Necrostatin-1, (n=3 for each group; *p<0.05, ***p<0.005; two-way ANOVA followed by Bonferroni post-test with alpha=5%).

(C, D) Representative EM images of wiltype control and *mdx* MuSCs (MF = myofiber, H = compact heterochromatin, E = open euchromatin) (C) and quantified in (D) (n=3 for each group; ***p<0.005, two-way ANOVA followed by Bonferroni post-test with alpha=5%). Scale bar: 1 µm.

(E) Heatmap representing gene expression of deregulated genes (DEGs) (Log2 expression) in MuSC from transwell-assay. WT MuSCs co-cultured with *mdx* or *mdx*/*Ripk3*^{mKO} were subjected to RNAseq analysis (n=2).

All analyses indicated across the experiments were biological replicates unless otherwise stated.

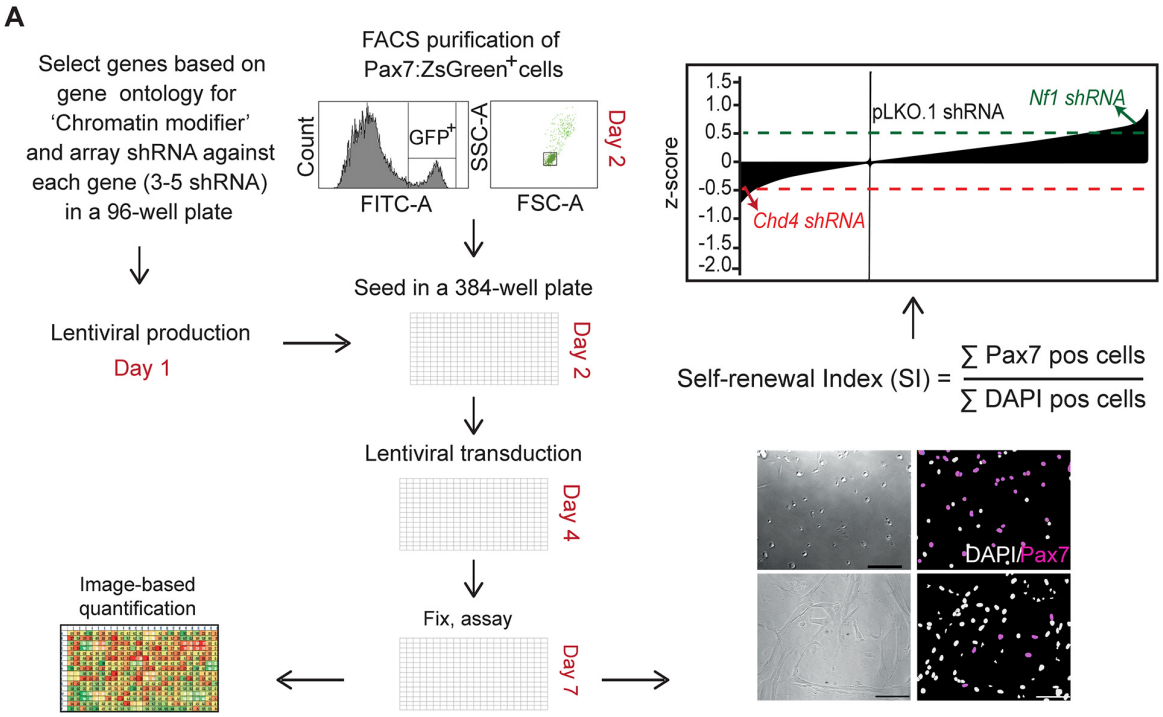

B

Increase of Pax7⁺ MuSCs	Decrease of Pax7⁺ MuSCs	Previously reported MuSC regulators
31/650 [5%]	27/650 [4%]	12/58 [20%]
shRNA targets Mbd1, Trp53, Cbx5, Suv39h2, AA619741	shRNA targets Chd4, Hdac2, Rbb4, Mta2 6330407J23Rik, 1700012L04Rik	shRNA targets Suv420h1, Hdac6, Ezh2, Ets2, Sirt1, Myocd, Sox15

C

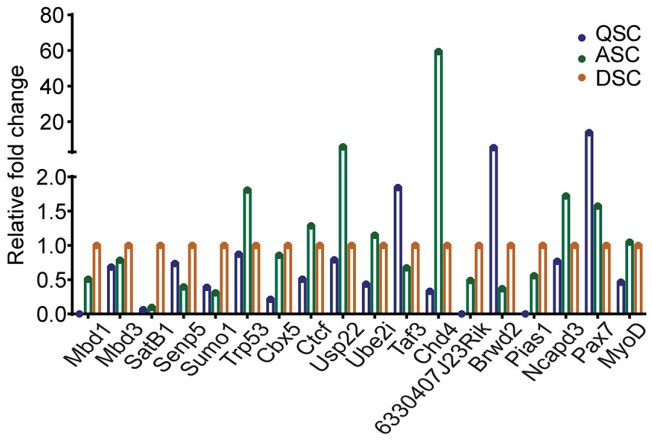

D

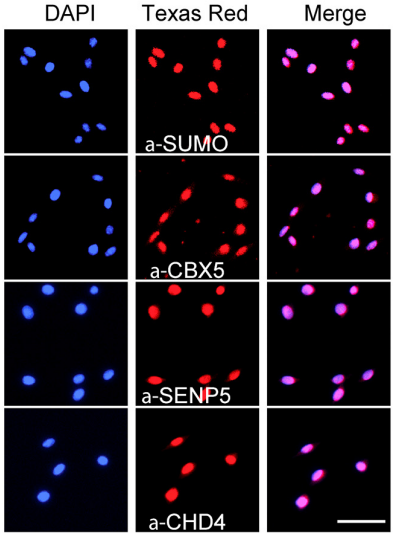

E

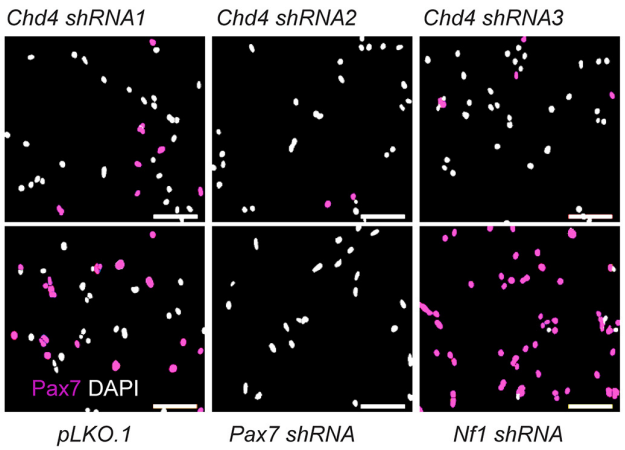

Supplemental Figure 3: Identification of chromatin modifiers regulating survival and expansion of MuSC by an shRNA screen. Related to Figure 4.

(A) Schematic representation of the shRNA screen for chromatin modifiers in MuSC.

(B) Novel and previously identified chromatin modifiers regulating MuSC survival and proliferation.

(C, D) RT-qPCR (C) and immunofluorescence analysis (activated MuSCs) (D) of expression of candidate genes regulating MuSC function (QSC = freshly isolated, ASC= Activated, DSC = Differentiated MuSC). Scale bar (D): 100 μm.

(E) Secondary validation of the role of Chd4 by shRNA mediated knockdown. shRNAs against *Pax7* and *Nf1* served as controls. Scale bar: 100 μm.

All analyses indicated across the experiments were biological replicates unless otherwise stated.

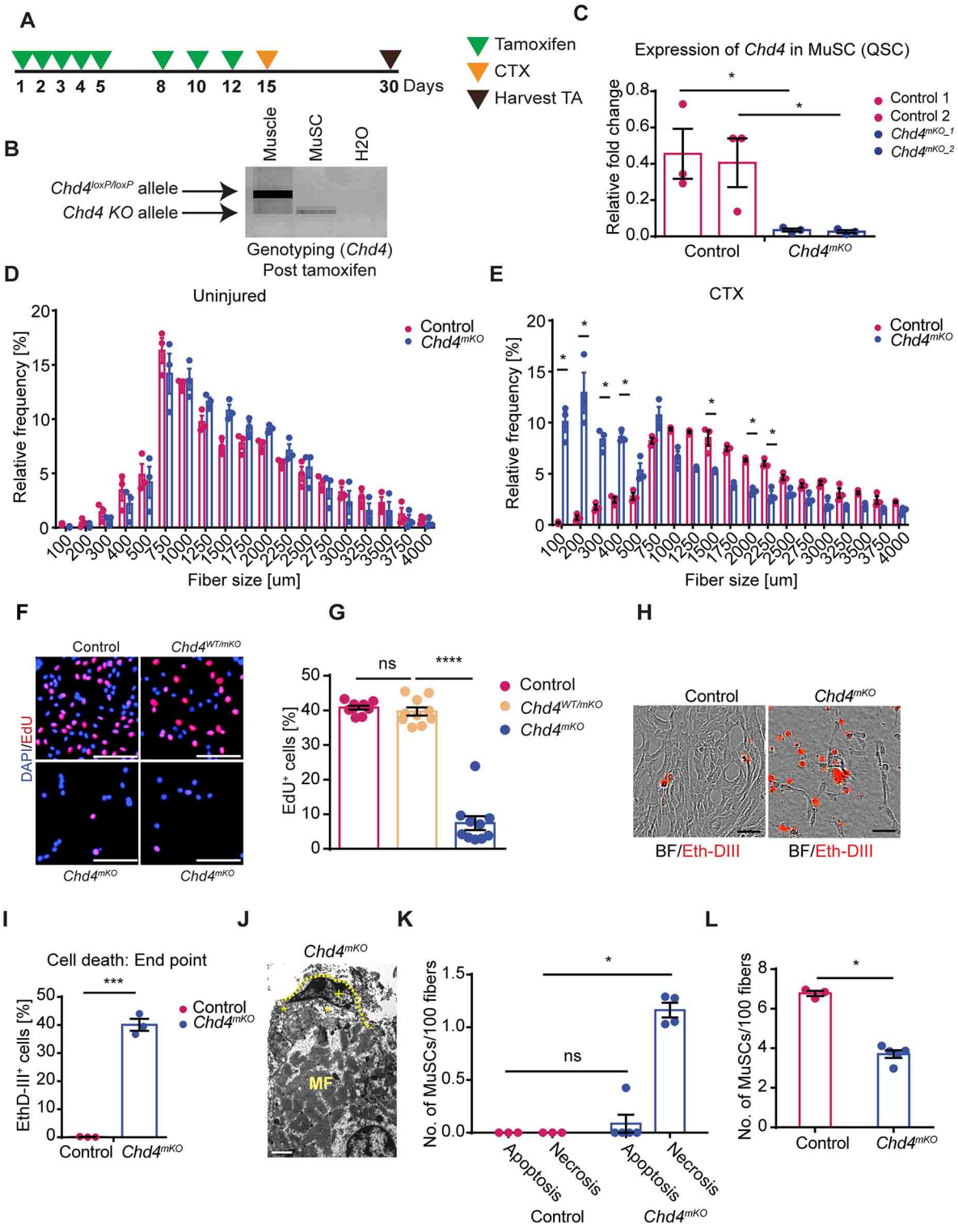

Supplemental Figure 4: ***Chd4* is required for skeletal muscle regeneration. Related to Figure 4.**

(A) Schematic representation of the tamoxifen treatment regiment, CTX injury and time point of TA muscle collection.

(B) PCR-based genotyping of skeletal muscle and MuSC purified from *Chd4*^{mKO} mice after tamoxifen treatment.

(C) RT-qPCR analysis of *Chd4* expression in MuSC from control and Chd4^{mKO} mice (n=3 for each group).

(D-E) Relative frequency of muscle fiber sizes in TA muscles from control and *Chd4*^{mKO} mice (n=3 for each group; *p<0.05; two-way ANOVA followed by Bonferroni post-test with alpha=5%).

(F, G) Representative images and quantification of EdU incorporation in cultured MuSC from control, $Chd4^{mKO/+}$ and $Chd4^{mKO}$ muscles (n=10 for each group). Scale bar: 100 μm.

(H, I) Analysis of EthD-III-incorporating necroptotic MuSC derived from control and $Chd4^{mKO}$ mice in culture (n=3 for each group). Scale bar: 100 μm.

(J) Representative EM micrograph of necrotic MuSC in TA muscles of $Chd4^{mKO}$ mice (MF = myofiber, + = intact chromatin/nucleus (necrosis), * = MuSC distrupted membrane). Scale bar: 1 μm.

(K, L) Quantification of apoptotic and necrotic MuSC in control (n=3-5) and $Chd4^{mKO}$ muscles (n=5) by EM (*$p<0.05$, ***$p<0.005$, ****$p< 0.001$; two-way ANOVA followed by Bonferroni post-test with alpha=5%).

All analyses indicated across the experiments were biological replicates unless otherwise stated.

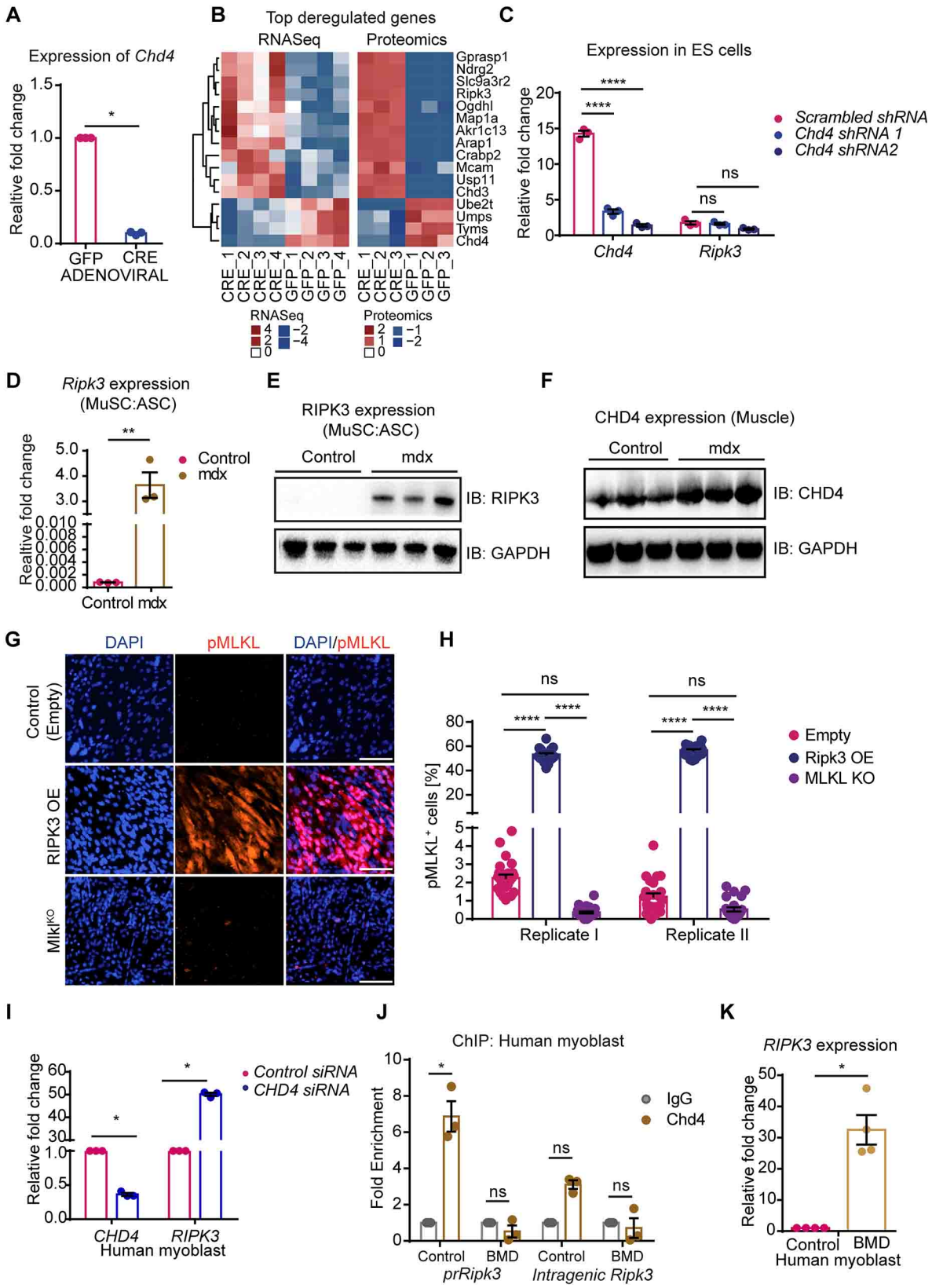

Supplemental Figure 5: **Upregulation of *Ripk3* in *mdx* MuSC is sufficient to induce necroptosis. Related to Figure 5.**

(A) RT-qPCR analysis of *Chd4* expression after Adeno-cre and Adeno-GFP infections of MuSC from *Chd4*$^{loxP/loxP}$ mice (n=4 for each group).

(B) Heatmap representation of gene expression of top 10 deregulated genes following adenoviral infection of MuSC from *Chd4*$^{loxP/loxP}$ mice.

(C) RT-qPCR analysis of *Chd4* and *Ripk3* expression in ESCs after shRNA mediated knockdown of *Chd4*.

(D, E) RT-qPCR and Western blot analysis of Ripk3 expression in MuSC from control and *mdx* mice (n=3 for each group).

(F) Western blot analysis of CHD4 expression in muscle tissues from control and *mdx* mice (n=3 for each group). (G) Immunofluorescence staining for pMLKL of proliferating WT MuSCs transduced with control (empty vector) and RIPK3OE (Ripk3-expression vector) lentiviral vectors. MuSC from $MLKL^{KO}$ mice ($MLKL^{-/-}$) were used as a negative control. Scale bar: 100 μm.

(H) Quantification of $pMLKL^{+}$ MuSC undergoing necroptosis (n=25 view fields in each of two independent lentiviral transduction). (*p<0.05, **p<0.01, ***p<0.005, ****p< 0.001; two-way ANOVA followed by Bonferroni post-test with alpha=5%).

I) RT-qPCR analysis of *Chd4* and *Ripk3* expression in human myoblasts after shRNA mediated knockdown of *Chd4*.

(J) ChIP-qPCR analysis of CHD4 binding to the promoter and intragenic regions of the *Ripk3* gene in myoblasts from heathy human controls and BMD patients. (K) RT-qPCR analyses of Ripk3 expression in myoblasts from heathy human controls and BMD patients. (in J and K: n=3 for each group; *p<0.05, **p<0.01, ***p<0.005; two-way ANOVA followed by Bonferroni post-test with alpha=5%).

All analyses indicated across the experiments were biological replicates unless otherwise stated.

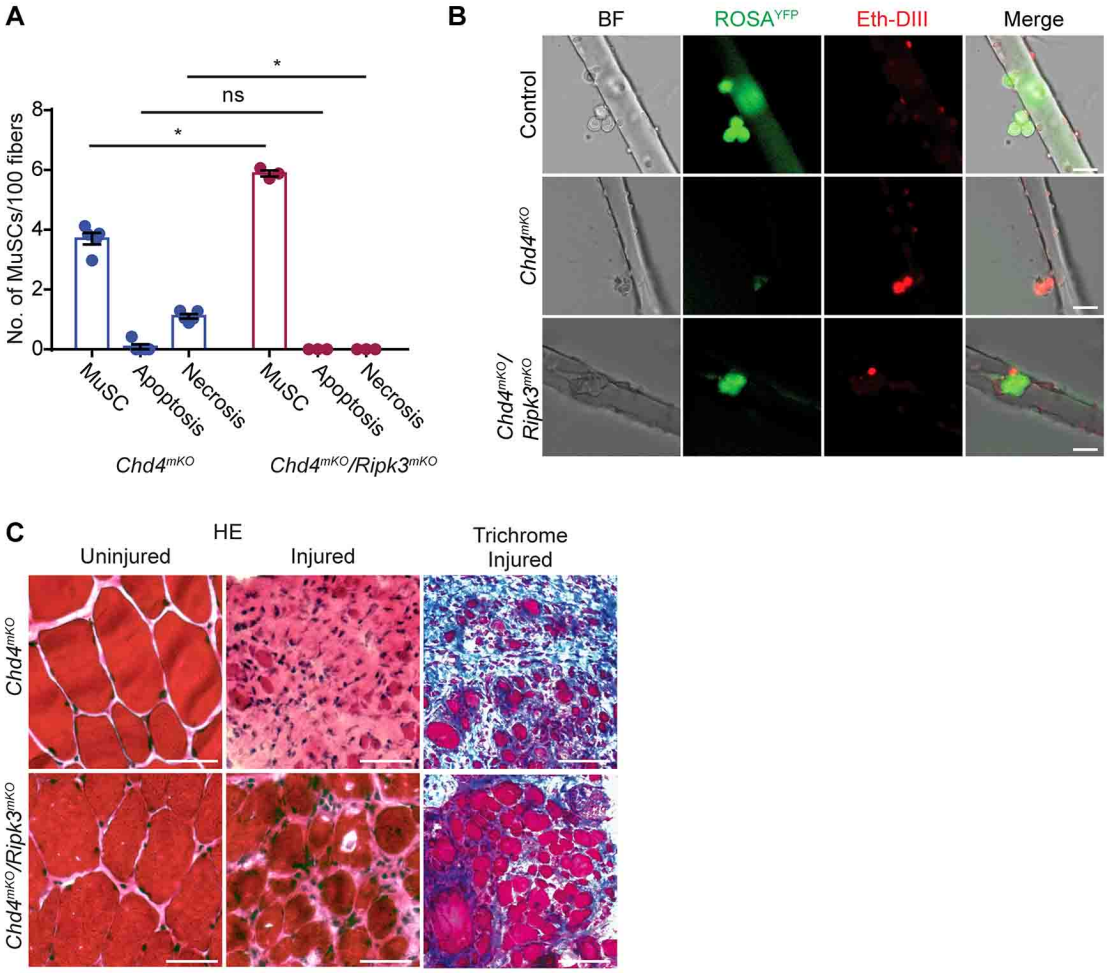

Supplemental Figure 6: Inhibition of necroptosis by inactivation of *Ripk3* in *Chd4^{mKO}* MuSC improves muscle regeneration. Related to Figure 6.

(A) Quantification of MuSC undergoing apoptosis and necroptosis in *Chd4^{mKO}*and *Chd4^{mKO}/Ripk3^{mKO}* mice based on EM analysis (n=3 each; *p<0.05; two-way ANOVA followed by Bonferroni post-test with alpha=5%).

(B) Images of *ex-vivo* cultured (day 3) single myofibers derived from Flexor Digitorum Brevis (FDB) muscles of control, *Chd4^{mKO}/ROSA26^{YFP}* and *Chd4^{mKO}/ROSA26^{YFP}/Ripk3^{mKO}* mice (n=3 for each group). Activation of the ROSA26^{YFP} reporter was used to monitor recombined MuSC. Incorporation of the EthD-III dye (red) labels cells undergoing necroptosis. Scale bar: 25 µm.

(C) Representative H&E and trichrome staining of TA muscle cross-sections from *Chd4^{mKO}* and *Chd4^{mKO}/Ripk3^{mKO}* mice. Scale bar: 100 µm.

All analyses indicated across the experiments were biological replicates unless otherwise stated.

Gene Name	Forward Primer	Reverse Primer
ChIP qRT-PCR		
prRipk3 (-963 to -766)	TGCCGCTTAGTAGGCAAAAT	GGGTCAGTTTGTTCTCTGCTG
Intragenic Ripk3 (+ 1053 to +1262)	TGAGTTGCTGATGGGCAG	AGTGTAGACTTGGGACCA
qRT-PCR (Gene Expression)		
Mbd1	GAGGACGAGCTACAGCCCTA	TTGCCACCCCCGAATTTGG
Mbd3	CCCCAGCGGGAAGAAGTTC	CGGAAGTCGAAGGTGCTGAG
SatB1	CATGTTACCAGTTTTCTGCGTG	GTGAATAGCCTAGAGACAGCAAC
Senp5	CCCCAAAACTTGTGCTTTCTGA	AGTAGCCAGTCCAGACTTTGT
Sumo1	ATTGGACAGGATAGCAGTGAGA	TCCCAGTTCTTTCGGAGTATGA
Trp53	GCGTAAACGCTTCGAGATGTT	TTTTTATGGCGGGAAGTAGACTG
Cbx5	GACAGGCGCATGGTTAAGG	CCTGGGCTTATTGTTTTCACCC
Ctcf	GATCCTACCCTTCTCCAGATGAA	GTACCGTCACAGGAACAGGT
Usp22	CTCCCCACACATTCCATACAAG	TGGAGCCCACCCGTAAAGA
Ube2i	TCATCCAAACGTGTATCCTTCTG	CTTGTGCTCGGACCCTTTTCT
Taf3	TGAGAACTTCTTGGGTAAGAGGC	TAGGGAGTCCCCTTTAGTGCT
Chd4	GAAATTGCTGCGGCACCATTA	AGCCATCATTGTAGTTGACCTG
Brwd2	CCCTACACCGTAAACTTCAAGG	ACTACCACCAGTGAATGGCAT
6330407J23Rik	GACGACAATGAGGATCTCAAGTG	TGCTTCTCCTTTGGGTAGAGG
Pias1	GCGGACAGTGCGGAACTAAA	ATGCAGGGCTTTTGTAAGAAGT
Ncapd3	TCTCAGCCTCGAATGGGTGAA	CTCTTCCAGTCTCTAGGATCTCG
Pax7	TCTCCAAGATTCTGTGCCGAT	CGGGGTTCTCTCTCTTATACTCC
MyoD	CCACTCCGGGACATAGACTTG	AAAAGCGCAGGTCTGGTGAG
Ripk3	TCTGTCAAGTTATGGCCTACTGG	GGAACACGACTCCGAACCC
m36B4	AGATTCGGGATATGCTGTTGGC	TCGGGTCCTAGACCAGTGTTC
Genotyping primer		
Pax7 CreERT2	ACTAGGCTCCACTCTGTCCTTC	GCAGATGTAGGGACATTCCAGTG
Pax7 Cre WT	GCTCTGGATACACCTGAGTCT	TCGGCCTTCTTCTAGGTTCTGCTC
Pax7 Cre MT	TCGGCCTTCTTCTAGGTTCTGCTC	GGATAGTGAAACAGGGGCAA
ZsGreen	CTGCATGTACCACGAGTCCA	GTCAGCTGCCACTTCTGGTT
ROSA-YFP	AAAGTCGCTCTGAGTTGTTAT	GGAGCGGGAGAAATGGATATG
Mdx WT	GCGCGAAACTCATCAAATATGCGTGTTAGTGT	GATACGCTGCTTTAATGCCTTTAGTCACTCAGATAGTTGAAGCCATTTTG
Mdx MT	GCGCGAAACTCATCAAATATGCGTGTTAGTGT	CGGCCTGTCACTCAGATAGTTGAA
Chd4loxP	CTCCAAGAAGAAGACGGCAGATCT	GTCCTTCCAAGAAGAGCAAG
Chd4KO	CTCCAAGAAGAAGACGGCAGATCT	CTTCCACAGTGACGTCCAGACGCA
Ripk3loxP	GATCCAGAGCTCCACGCCAAG	TGGAGGACCAGAGGGAAGGT

Supplementary Table 5 (Related to STAR methods).

List of primer sequences used in the study.